Ocean Systems Engineering, *Vol. 6, No. 4 (2016) 363-375*
DOI: http://dx.doi.org/10.12989/ose.2016.6.4.363

A hybrid method for predicting the dynamic response of free-span submarine pipelines

Tongtong Li[1,2], Menglan Duan[1], Wei Liang[2] and Chen An[*1]

[1]*Institute for Ocean Engineering, China University of Petroleum, Beijing, 102249, China*
[2]*College of Mechanical and Transportation Engineering, China University of Petroleum, Beijing, 102249, China*

(Received October 22, 2015, Revised October 8, 2016, Accepted October 13, 2016)

Abstract. Large numbers of submarine pipelines are laid as the world now is attaching great importance to offshore oil exploitation. Free spanning of submarine pipelines may be caused by seabed unevenness, change of topology, artificial supports, etc. By combining Iwan's wake oscillator model with the differential equation which describes the vibration behavior of free-span submarine pipelines, the pipe-fluid coupling equation is developed and solved in order to study the effect of both internal and external fluid on the vibration behavior of free-span submarine pipelines. Through generalized integral transform technique (GITT), the governing equation describing the transverse displacement is transformed into a system of second-order ordinary differential equations (ODEs) in temporal variable, eliminating the spatial variable. The MATHEMATICA built-in function *NDSolve* is then used to numerically solve the transformed ODE system. The good convergence of the eigenfunction expansions proved that this method is applicable for predicting the dynamic response of free-span pipelines subjected to both internal flow and external current.

Keywords: free-span submarine pipeline; vortex-induced vibration; internal flow; integral transform; pinned-pinned

1. Introduction

The crucial works of a small number of disparate researchers in the late 19th and early 20th centuries marked the beginnings of a concerted attempt to understand the phenomenon of vortex shedding which continues to this day. A great amount of work has been done to study the vortex-induced vibration (VIV) behavior of underwater structures, such as cable arrays, drilling risers, offshore platforms and pile-supported structures.

During the early days, the effect of the internal flow was often ignored. Iwan (1981) proposed a vortex-induced oscillation model that can be used to solve problems involving non-uniform structures and flow profiles. Xu, Lauridsen *et al*. (1999) developed the fatigue damage models for multi-span pipelines detailed both in time and frequency domain approaches. Pantazopoulos, Crossley *et al*. (1993) put forward a Fourier Transformation based methodology to study the VIV of free-span submarine pipelines. Bryndum and Smed (1998) carried experiments in the VIV of submarine free spans under different boundary conditions. Furnes (2003) formulated time domain

∗Corresponding author, E-mail: tong-tong.li10@alumni.imperial.ac.uk

http://www.techno-press.org/?journal=ose&subpage=7 ISSN: 2093-6702 (Print), 2093-677X (Online)

model of a free-span pipeline subjected to ocean currents where the in-line and cross-flow deflections are coupled.

Recently, a significant number of achievements have been gained in understanding the dynamic characteristics of submarine risers and pipelines conveying internal fluid. Shen and Zhao (1996) studied the impact of internal fluid on the fatigue life of submarine pipelines under vortex-induced vibration while simplifying the action of the external flow on the pipe as a type of load, and ignoring the coupling effect of the two. Guo, Wang *et al*. (2004) and Lou (2005) studied the coupled effect of internal and external fluid on the response of VIV of marine risers by using the method of Finite Element Method (FEM).

In addition, an increasing amount of interest is paid to the phenomenon of VIV that concerns the influence of soil. Xing, Liu *et al*. (2005) developed a VIV model for the span segment of buried submarine pipelines. In an experimental study conducted by Yang, Gao *et al.* (2008), the cross-line VIV of a submarine pipeline near an erodible sandy seabed under the influence of ocean currents was investigated. By using Visual Basic tools, Xie, Chen *et al*. (2011) developed a VIV fatigue analysis program for submarine pipeline span based on a non-linear pipe-soil coupling modal. Wang, Tang *et al*. (2014) proposed a prediction model for the VIV of deepwater steel catenary risers considering the riser-seafloor interaction.

Finite Difference Method (FDM), Finite Element Method (FEM) and some other methods have been taken for the numerical solution of coupled nonlinear oscillator models. However, there exist no previous researches adopting the generalized integral transform technique (GITT) approach to solve such coupled fluid and structural equations. GITT is still in its starting stage in the area of structure mechanics. Ma, Su *et al*. (2006) applied GITT to solve a transverse vibration problem of an axial moving string and the convergence behavior of integral transform solution was examined. An and Su (2011, 2014) employed GITT to obtain a hybrid analytical-numerical solution for dynamic response of clamped axially moving beams, and afterwards the axially moving Timoshenko beams. Recently, Gu, An *et al*. (2012, 2013) used GITT to prove that variation of mean axial tension induced by elongation should not be neglected in the numerical simulation of VIV of a long flexible cylinder, and in addition, they predicted that the dynamic response of a clamped-clamped pipe conveying fluid, where the convergence behavior was thoroughly examined.

It is against this backdrop that the research presented in this article was undertaken. To this end, the remainder of this paper is organized as follows. In Section 2, the mathematical model of the coupled structure and wake oscillator model is put forward. In Section 3, the hybrid numerical-analytical solution is obtained through integral transform. Section 4 presents the numerical results and parametric studies, where the convergence behavior of the present approach is assessed and the influence of some parameters are discussed. Finally, Section 5 concludes this article.

2. Description of mathematical model

As is shown in Fig. 1, a Cartesian coordinate system is adopted to depict the vibration behavior of a submarine free span under the influence of both the internal and external fluid. The *x*-axis is the initial axis of the pipe; the *y*-axis is in the same direction as the current, horizontally orthogonal to the *x*-axis; and the *z*-axis is in the opposite direction of gravity. Consider a free-span pipeline that is horizontally pinned at $x=0$ and $x=L$. The pipeline is cylindrical with a constant outer diameter D and inner diameter D_i. The axial tension is T_a and the internal pressure is P. Assume that:

(1) The internal fluid flows at a constant velocity of V.

(2) The effect of waves is ignored and the current is at a constant speed of U.

(3) The property of the pipe is linear and the pipe is elastic.

Considering the movement of the free-span pipeline with pinned-pinned boundary conditions in the xoz plane subject to internal and external fluid, tension and the pressure from the internal fluid, according to Guo, Wang *et al*. (2004), Lou, Ding *et al*. (2005) and Faccinetti, Langrea *et al*. (2004), the coupled structure and wake oscillator model of the pipe vibration can be described as

$$\begin{cases} EI\dfrac{\partial^4 z}{\partial x^4}+(m_iV^2+PA_i-T_a)\dfrac{\partial^2 z}{\partial x^2}+2m_iV\dfrac{\partial^2 z}{\partial x\partial t}+(r_s+r_f)\dfrac{\partial z}{\partial t}+m\dfrac{\partial^2 z}{\partial t^2}=\dfrac{\rho_e U^2 DC_L}{2} \\ \dfrac{\partial^2 q}{\partial t^2}+\varepsilon w_f(q^2-1)\dfrac{\partial q}{\partial t}+w_f{}^2 q=\dfrac{\alpha}{D}\dfrac{\partial^2 z}{\partial t^2} \end{cases} \quad (1)$$

The model here is constraint to cross-flow vibrations, where,

EI -- flexural stiffness; P -- internal pressure; Ai -- area of the inner cross section of the pipeline; T_a -- axial tension; ρ_e -- density of external fluid; D -- outside diameter of the pipeline; D_i -- inner diameter of the pipeline; r_s -- structural damping; r_f -- fluid added damping, equaling to $\Upsilon w_f \rho_e D^2$, of which Υ is a coefficient related to the mean sectional drag efficient of the pipe - C_D, and $\Upsilon = C_D/(4\pi St)$ (here St is the Strouhal number); and for unit length of the pipeline, $m = m_i + m_p + m_e$, with m_i being the internal fluid mass, m_p being the mass of the pipeline, m_e being the added mass due to external fluid, and $m_e = C_M \rho_e D^2/4$, in which C_M is the added mass coefficient; q is the reduced fluctuating lift coefficient, and $q(x,t) = 2C_L(x,t)/C_{L0}$, and C_L is the lift coefficient, C_{L0} the reference lift coefficient which can be obtained from observation of a fixed structure subject to vortex shedding; $w_f = 2\pi StU/D$ denotes the vortex-shedding frequency; parameters α and ε can be derived from experimental results by Faccinetti, Langrea *et al*. (2004), with the former being 12 and the latter 0.3.

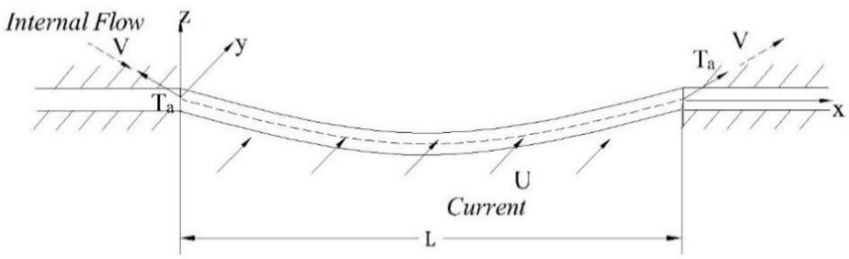

Fig. 1 Free Span of a Submarine Pipeline

As the free span considered in this article is pinned-pinned, the boundary conditions is as follows

$$z(0,t)=0,\ \frac{\partial^2 z(0,t)}{\partial x^2}=0,\ z(L,t)=0,\ \frac{\partial^2 z(L,t)}{\partial x^2}=0 \tag{2a}$$

$$q(0,t)=0,\ \frac{\partial^2 q(0,t)}{\partial x^2}=0,\ q(L,t)=0,\ \frac{\partial^2 q(L,t)}{\partial x^2}=0 \tag{2b}$$

Then the following dimensionless variables are introduced

$$x^*=\frac{x}{L},\ z^*=\frac{z}{D},\ t^*=\frac{t}{L^2}\sqrt{\frac{EI}{m_p}},\ V^*=VL\sqrt{\frac{m_p}{EI}},\ U^*=UL\sqrt{\frac{m_p}{EI}},\ w_f{}^*=w_f L^2\sqrt{\frac{m_p}{EI}},\ \beta=\frac{\rho_e U^2 C_{L0} L^4}{4EI} \tag{3}$$

By combining Eq. (3) into Eq. (1), two dimensionless equations are obtained (leaving out the asterisks for simplicity)

$$\begin{cases} \dfrac{\partial^4 z}{\partial x^4}+(\dfrac{m_i V^2}{m_p}+\dfrac{PA_i L^2}{EI}-\dfrac{T_a L^2}{EI})\dfrac{\partial^2 z}{\partial x^2}+\dfrac{2m_i V}{m_p}\dfrac{\partial^2 z}{\partial x \partial t}+(r_s+r_f)\dfrac{L^2}{\sqrt{m_p EI}}\dfrac{\partial z}{\partial t}+\dfrac{m}{m_p}\dfrac{\partial^2 z}{\partial t^2}=\beta q \\ \dfrac{\partial^2 q}{\partial t^2}+\varepsilon w_f (q^2-1)\dfrac{\partial q}{\partial t}+w_f{}^2 q=\alpha\dfrac{\partial^2 z}{\partial t^2} \end{cases} \tag{4}$$

along with the boundary conditions being changed to

$$z(0,t)=0,\ \frac{\partial^2 z(0,t)}{\partial x^2}=0,\ z(1,t)=0,\ \frac{\partial^2 z(1,t)}{\partial x^2}=0 \tag{5a}$$

and

$$q(0,t)=0,\ \frac{\partial^2 q(0,t)}{\partial x^2}=0,\ q(1,t)=0,\ \frac{\partial^2 q(1,t)}{\partial x^2}=0 \tag{5b}$$

The initial conditions is defined as

$$z(x,0)=0,\ \frac{\partial z(x,0)}{\partial t}=0,\ q(x,0)=1,\ \frac{\partial q(x,0)}{\partial t}=0 \tag{6}$$

3. Integral transform solution

According to the idea of GITT, the next step is to select the auxiliary eigenvalue problem and propose the eigenfunction expansion for Eq. (4) under the boundary conditions (5). For the transverse displacement of a free span, the eigenvalue problem is chosen as

$$\frac{\mathrm{d}^4 X_i(x)}{\mathrm{d}x^4}=\phi_i^4 X_i(x),\quad 0<x<1 \tag{7a}$$

with the boundary conditions being

$$X_i(0)=0\,,\ \ \frac{\mathrm{d}^2 X_i(0)}{\mathrm{d}\,x^2}=0\,,\ \ X_i(1)=0\,,\ \ \frac{\mathrm{d}^2 X_i(1)}{\mathrm{d}\,x^2}=0 \tag{7b}$$

where X_i and ϕ_i are respectively the eigenfunction and the eigenvalue of problem (7), satisfying the following orthogonality

$$\int_0^1 X_i(x)X_j(x)\,\mathrm{d}\,x=\delta_{ij}N_i \tag{8}$$

where δ_{ij} is the Kronecker delta, and for $i\neq j$, $\delta_{ij}=0$; for $i=j$, $\delta_{ij}=1$.

The normalization integral is evaluated as

$$N_i=\int_0^1 X_i^{\,2}(x)\,\mathrm{d}\,x \tag{9}$$

Problem (7) is now readily solved analytically to yield

$$X_i(x)=\sin(\phi_i x) \tag{10}$$

where the eigenvalue is obtained by

$$\phi_i=i\pi,\ \ i=1,2,3... \tag{11}$$

and the normalization integral is evaluated as

$$N_i=\frac{1}{2},\ \ i=1,2,3... \tag{12}$$

Therefore, in this case, the normalised eigenfunction coincides with the original eigenfunction itself, i.e.

$$\tilde{X}_i(x)=\frac{X_i(x)}{N_i^{1/2}} \tag{13}$$

This solution proceeds by putting forward the integral transform pair – the integral transformation itself and the inversion formula. Through integral transform, the spatial coordinate x is eliminated.

For the transverse displacement

$$\bar{z}_i(t)=\int_0^1 \tilde{X}_i(x)z(x,t)\,\mathrm{d}\,x\text{, transform} \tag{14a}$$

$$z(x,t)=\sum_{i=1}^{\infty}\tilde{X}_i(x)\bar{z}_i(t)\text{, inversion} \tag{14b}$$

Similarly, the eigenvalue problem is chosen for $q(x,t)$ is

$$\frac{\mathrm{d}^4 Y_k(x)}{\mathrm{d}\,x^4}=\varphi_k^{\,4}Y_k(x)\,,\ \ 0<x<1 \tag{15a}$$

with the boundary conditions being

$$Y_k(0)=0,\ \frac{\mathrm{d}^2 Y_k(0)}{\mathrm{d}x^2}=0,\ Y_k(1)=0,\ \frac{\mathrm{d}^2 Y_k(1)}{\mathrm{d}x^2}=0 \tag{15b}$$

where Y_k is the eigenfunction of problem (15) and φ_k the corresponding eigenvalue. And similarly

$$\int_0^1 Y_k(x)Y_l(x)\,\mathrm{d}x=\delta_{kl}N_k \tag{16}$$

The same mathematical manipulation is carried here as Eqs. (8)-(13), and the eigenvalue problem (15) defines the integral transform pair for the wake variable as follows

$$\bar{q}_k(t)=\int_0^1 \tilde{Y}_k(x)q(x,t)\,\mathrm{d}x,\ \text{transform} \tag{17a}$$

$$q(x,t)=\sum_{k=1}^{\infty}\tilde{Y}_k(x)\bar{q}_k(t),\ \text{inversion} \tag{17b}$$

To perform GITT, the dimensionless equation system (4) is multiplied by operators $\int_0^1 \tilde{X}_i(x)\,\mathrm{d}x$ and $\int_0^1 \tilde{Y}_k(x)\,\mathrm{d}x$, and also the inverse formula (14) and (17) are applied, resulting in a set of ordinary differential equations

$$\begin{cases}\phi_i^4\bar{z}_i(t)+\left(\frac{m_iV^2}{m_p}+\frac{PA_iL^2}{EI}-\frac{T_aL^2}{EI}\right)\sum_{j=1}^{\infty}A_{ij}\bar{z}_j(t)+\frac{2m_iV}{m_p}\sum_{j=1}^{\infty}B_{ij}\frac{\mathrm{d}\bar{z}_j(t)}{\mathrm{d}t}+(r_s+r_f)\frac{L^2}{\sqrt{EIm_p}}\frac{\mathrm{d}\bar{z}_i(t)}{\mathrm{d}t}\\ +\frac{m}{m_p}\frac{\mathrm{d}^2\bar{z}_i(t)}{\mathrm{d}t^2}=\beta\sum_{k=1}^{\infty}C_{ik}\bar{q}_k(t)\\ \frac{\mathrm{d}^2\bar{q}_k(t)}{\mathrm{d}t^2}+\varepsilon w_f\sum_{l=1}^{\infty}\sum_{r=1}^{\infty}\sum_{s=1}^{\infty}D_{klrs}\bar{q}_l(t)\bar{q}_r(t)\frac{\mathrm{d}\bar{q}_s(t)}{\mathrm{d}t}-\varepsilon w_f\frac{\mathrm{d}\bar{q}_k(t)}{\mathrm{d}t}+w_f^{\,2}\bar{q}_k(t)=\alpha\sum_{i=1}^{\infty}E_{ki}\frac{\mathrm{d}^2\bar{z}_i(t)}{\mathrm{d}t^2}\end{cases} \tag{18}$$

where the coefficients are analytically determined by the following integrals

$$A_{ij}=\int_0^1\tilde{X}_i(x)\frac{\mathrm{d}^2\tilde{X}_j(x)}{\mathrm{d}x^2}\mathrm{d}x,\ B_{ij}=\int_0^1\tilde{X}_i(x)\frac{\mathrm{d}\tilde{X}_j(x)}{\mathrm{d}x}\mathrm{d}x,\ C_{ik}=\int_0^1\tilde{X}_i(x)\tilde{Y}_k(x)\,\mathrm{d}x,$$

$$D_{klrs}=\int_0^1\tilde{Y}_k(x)\tilde{Y}_l(x)\tilde{Y}_r(x)\tilde{Y}_s(x)\,\mathrm{d}x,\ E_{ki}=\int_0^1\tilde{Y}_k(x)\tilde{X}_i(x)\,\mathrm{d}x \tag{19}$$

In a similar manner, the boundary and the initial conditions are also transformed to omit the spatial variable, yielding

$$\bar{z}_i(0)=0,\ \frac{\mathrm{d}^2\bar{z}_i(0)}{\mathrm{d}t^2}=0,\ \bar{q}_k(0)=0,\ \frac{\mathrm{d}^2\bar{q}_k(0)}{\mathrm{d}t^2}=0,\ i,k=1,2,3\ldots \tag{20a}$$

and

$$\bar{z}_i(0)=0,\ \frac{\mathrm{d}^2\bar{z}_i(0)}{\mathrm{d}t^2}=0,\ \bar{q}_k(0)=\int_0^1\tilde{Y}_k(x)\,\mathrm{d}\,x,\ \frac{\mathrm{d}\bar{q}_k(0)}{\mathrm{d}t}=0,\ i,k=1,2,3... \tag{20b}$$

For computational purposes, the expansions for the transverse displacement $z(x,t)$ and the reduced lift coefficient $q(x,t)$ are truncated to finite *N* order. The equation system (18), in truncated series, are subsequently calculated by the *NDSolve* routine of MATHEMATICA. Once $\bar{z}_i(t)$ and $\bar{q}_k(t)$ are numerically evaluated, the inversion formulas Eqs. (14) and (17) are than applied in order that the explicit analytical expressions for the dimensionless $z(x,t)$ and $q(x,t)$ are obtained.

4. Results and discussion

In this Section, the numerical results of the transverse displacement $z(x,t)$ of a free-span submarine pipeline subject to both internal and external fluid under pinned-pinned boundary condition are presented.

The main parameters used in the present work is set as follows

Assume $P = 0$, $T_a = 50\ kN$. The dimensionless transverse deflection $z(x,t)$ is calculated with two different values of dimensionless internal fluid velocity, i.e., $V = 0.5, 1$, and two different values of dimensionless current velocity, i.e., $U = 0.05, 0.1$. The convergence behavior of the integral transform solution is examined for an increasing truncation terms $N = 4, 8, 16, 24$ at $t = 5, 20, 50$. The results of (i) $V = 0.5, U = 0.05$, (ii) $V = 1, U = 0.05$, (iii) $V = 0.5, U= 0.1$, and (iv) $V = 1, U = 0.1$, are displayed in Tables 2 and 3. Results show that convergence can be achieved even with a low truncation order ($N \geq 16$). (See Tables 2 and 3)

The Figs. 2-4 present respectively the GITT solution for the dimensionless $z(x,t)$ under different internal and external fluid velocities in 3-D diagrams; the time history curve and the corresponding frequency domain analysis of the vibration of the span midpoint; and the configuration of the free span at t = 25. Results gives that the maximum displacement-to-diameter ratio of the above mentioned situations i.e. (i) $V = 0.5, U = 0.05$, (ii) $V = 1, U = 0.05$, (iii) $V = 0.5, U= 0.1$, and (iv) $V = 1, U = 0.1$, respectively are 0.5022, 0.5191, 0.3089, 0.2771. Frequency analysis indicates that there is only one single mode contributing to the vibration of the free span; and the change of internal flow velocity does not necessarily change the vibration amplitude of the pipeline significantly, while as the current velocity changes, the vibration amplitude also changes. However, in order to get a thorough understanding the mechanism of how both the internal flow and current impact the dynamic response of free-spanning pipelines, further studies need to be conducted in future.

Table 1 Main Parameters of the Pipeline and the Fluid

L (m)	D (m)	D_i (m)	ρ_p (kg/m^3)	ρ_e (kg/m^3)	ρ_i (kg/m^3)	EI (Nm^2)	C_M	C_D	C_{L0}	St
40	0.35	0.325	8200	1025	908.2	3.779×10^7	1	1.2	0.3	0.2

Table 2 Convergence Behavior of $z(x,t)$ for *V = 0.5, 1* and *U = 0.05*

V = 0.5; *U* = 0.05					*V* = 1; *U* = 0.05				
x	*N*=4	*N*=8	*N*=16	*N*=20	*x*	*N*=4	*N*=8	*N*=16	*N*=20
t=5					*t*=5				
0.1	-0.0836	-0.0846	-0.0848	-0.0848	0.1	-0.0604	-0.0611	-0.0612	-0.0612
0.3	-0.2197	-0.2220	-0.2225	-0.2225	0.3	-0.1610	-0.1627	-0.1630	-0.0614
0.5	-0.2732	-0.2761	-0.2766	-0.2766	0.5	-0.2042	-0.2065	-0.2069	-0.2069
0.7	-0.2228	-0.2252	-0.2257	-0.2257	0.7	-0.1701	-0.1720	-0.1723	-0.1723
0.9	-0.0857	-0.0866	-0.0868	-0.0868	0.9	-0.0663	-0.0672	-0.0673	-0.0673
t=20					*t*=20				
0.1	0.0540	0.0581	0.0600	0.0603	0.1	0.0397	0.0390	0.0384	0.0383
0.3	0.1392	0.1499	0.1550	0.1559	0.3	0.1093	0.1074	0.1059	0.1056
0.5	0.1675	0.1808	0.1871	0.1882	0.5	0.1448	0.1427	0.1409	0.1405
0.7	0.1311	0.1419	0.1469	0.1478	0.7	0.1258	0.1243	0.1229	0.1225
0.9	0.0488	0.0528	0.0547	0.0550	0.9	0.0505	0.0501	0.0496	0.0494
t=50					*t*=50				
0.1	0.0505	0.0426	0.0375	0.0364	0.1	-0.0485	-0.0531	-0.0557	-0.0562
0.3	0.1344	0.1136	0.1002	0.0974	0.3	-0.1217	-0.1339	-0.1407	-0.1421
0.5	0.1706	0.1449	0.1285	0.0973	0.5	-0.1406	-0.1556	-0.1641	-0.1658
0.7	0.1423	0.1218	0.1085	0.1057	0.7	-0.1049	-0.1170	-0.1238	-0.1252
0.9	0.0557	0.0479	0.0429	0.0419	0.9	-0.0376	-0.0420	-0.0444	-0.0451

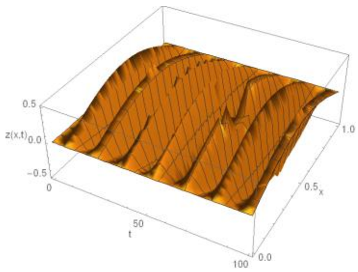

(a)

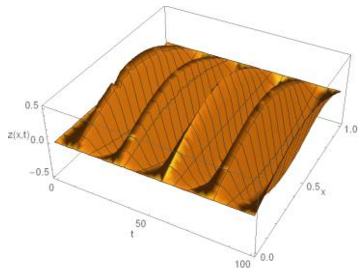

(b)

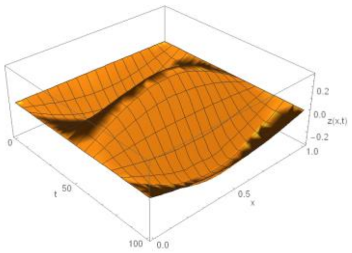

(c)

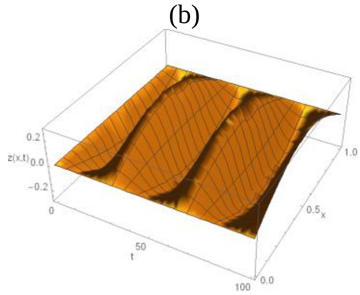

(d)

Fig. 2 GITT Solution for the dimensionless $z(x,t)$. (a) *V = 0.5, U = 0.05*, (b) *V = 1, U = 0.05*, (c) *V = 0.5, U= 0.1* and (d) *V = 1, U = 0.1* (*N* = 16)

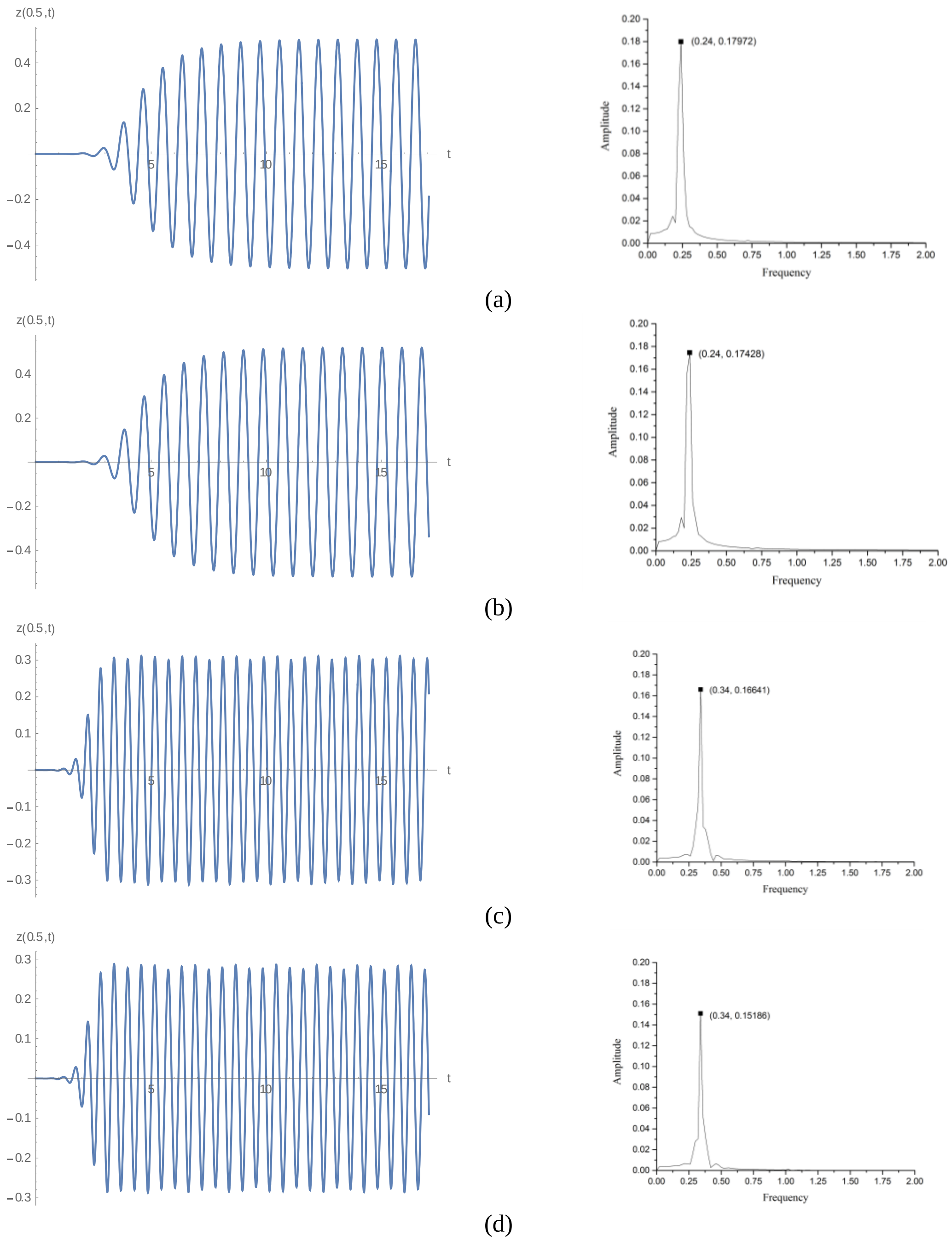

Fig. 3 Time history curve of the vibration of the span midpoint. (a) $V = 0.5$, $U = 0.05$, (b) $V = 1$, $U = 0.05$, (c) $V = 0.5$, $U = 0.1$ and (d) $V = 1$, $U = 0.1$ ($N = 16$)

Table 3 Convergence Behavior of $z(x,t)$ for *V = 0.5, 1* and *U = 0.1*

V = 0.5; *U* = 0.1					*V* = 1; *U* = 0.1				
x	*N*=4	*N*=8	*N*=16	*N*=20	*x*	*N*=4	*N*=8	*N*=16	*N*=20
t=5					*t*=5				
0.1	-0.0201	-0.0174	-0.0229	-0.0223	0.1	-0.0116	-0.0110	-0.0156	-0.0152
0.3	-0.0495	-0.0418	-0.0560	-0.0545	0.3	-0.0245	-0.0229	-0.0346	-0.0332
0.5	-0.0562	-0.0467	-0.0643	-0.0623	0.5	-0.0212	-0.0194	-0.0336	-0.0319
0.7	-0.0424	-0.0350	-0.0492	-0.0475	0.7	-0.0111	-0.0098	-0.0213	-0.0198
0.9	-0.0156	-0.0130	0.0186	-0.0179	0.9	-0.0029	-0.0026	-0.0071	-0.0065
t=20					*t*=20				
0.1	0.0227	0.0150	0.0673	0.0667	0.1	-0.0836	-0.0542	-0.0422	-0.0365
0.3	0.0562	0.0357	0.1736	0.1718	0.3	-0.2216	-0.1502	-0.1183	-0.1035
0.5	0.0645	0.0396	0.2117	0.2086	0.5	-0.2764	-0.1960	-0.1557	-0.1390
0.7	0.0491	0.0296	0.1687	0.1653	0.7	-0.2230	-0.1636	-0.1301	-0.1168
0.9	0.0181	0.0110	0.0639	0.0622	0.9	-0.0846	-0.0634	-0.0500	-0.0454
t=50					*t*=50				
0.1	0.0268	0.0466	0.0892	0.0869	0.1	0.0825	-0.0767	-0.0762	-0.0850
0.3	0.0672	0.1207	0.2373	0.2316	0.3	0.2192	-0.2010	-0.1967	-0.2219
0.5	0.0782	0.1469	0.2969	0.2908	0.5	0.2743	-0.2473	-0.2391	-0.2723
0.7	0.0602	0.1171	0.2398	0.2361	0.7	0.2215	-0.1985	-0.1898	-0.2179
0.9	0.0223	0.0445	0.0909	0.0901	0.9	0.0840	-0.0754	-0.0715	-0.0824

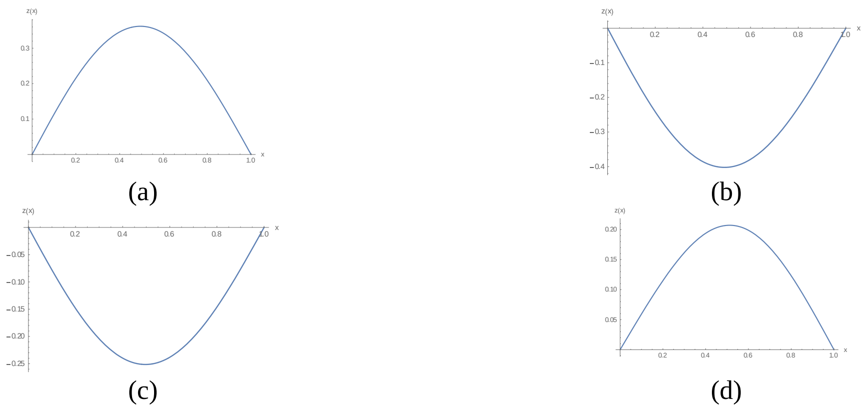

Fig. 4 Span configuration at t = 25. (a) *V = 0.5, U = 0.05*, (b) *V = 1, U = 0.05*, (c) *V = 0.5, U= 0.1* and (d) *V = 1, U = 0.1* (N = 16)

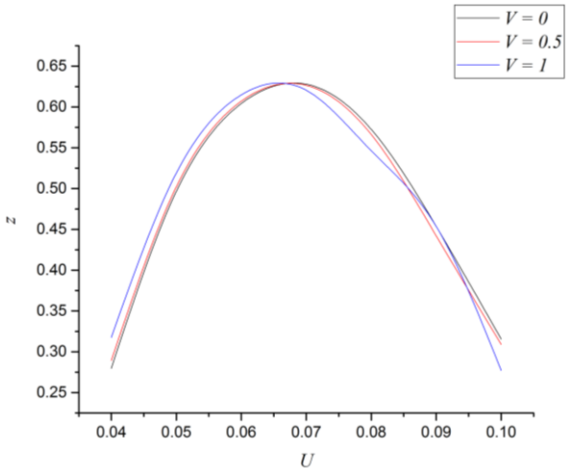

Fig. 5 Displacement-to-diameter ratio under different internal & external flow velocity (N = 16)

Fig. 5 shows the influence of different internal flow velocity on the vibration amplitude of the free span in cross-flow direction. When the dimensionless current velocity is low, the higher the internal flow velocity is, the larger the vibration amplitude of the span will be; on the contrary, when the dimensionless current velocity reaches a certain point, the higher the internal flow velocity is, the smaller the amplitude will be.

During the above mentioned calculation, the internal pressure is neglected. In fact, the internal pressure cannot simply be assumed to be zero. The influence of the internal pressure is calculated and manifested in Fig. 6. It shows that, as the internal pressure increases, the vibration amplitude of the free span midpoint also increases. However, the influence is quite subtle and can be ignored.

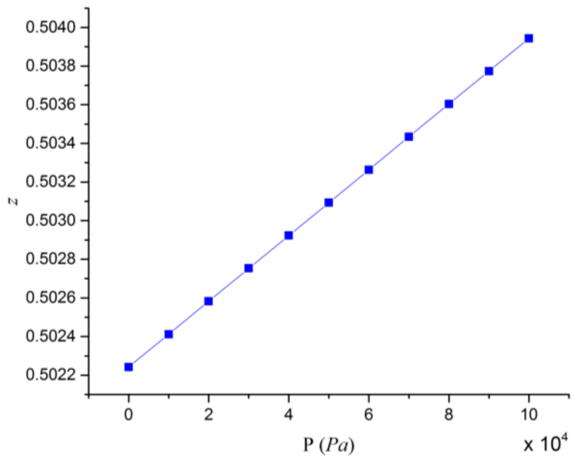

Fig. 6 Influence of the internal pressure on the displacement-to-diameter ratio at span midpoint with $V = 0.5$, $U = 0.05$ (N = 16)

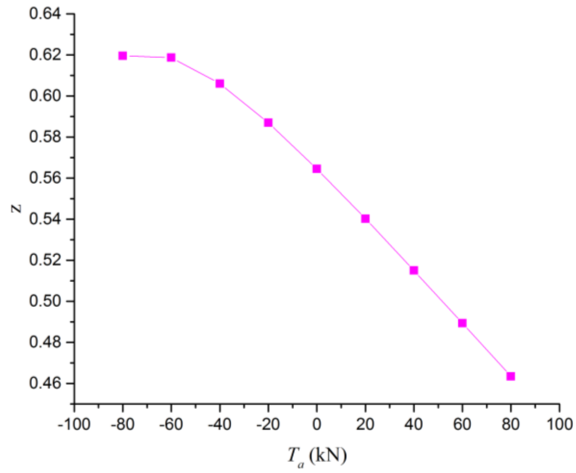

Fig. 7 Influence of the axial stress on the displacement-to-diameter ratio at span midpoint (N = 16)

In most cases, submarine pipelines are laid by pipe-laying vessel, and it is inevitable that pipelines are subject to the axial residual stress. The influence of the axial stress on the vibration of free-span pipelines are discussed below. Fig. 7 gives the results of how different axial stress affect the vibration amplitude of free spans. The dimensionless internal flow velocity and current velocity are 0.5 and 0.05 respectively, with the internal pressure taken as zero. Results show that, as the axial tension ($T_a > 0$) increases, the vibration amplitude of the free span midpoint decreases, while as the axial pressure ($T_a < 0$) increases, the vibration amplitude also increases.

5. Conclusions

It is proved in the present studies that GITT is feasible and fast approach for analyzing the dynamic response of free-span submarine pipelines under the influence of both the external current and the internal flow. This method can be employed for benchmarking purposes, yielding sets of reference results with controlled accuracy. Due to the limit of time, this article only cover the work presented above. It is suggested that results are to be verified against previous literature or by other methodologies.

Acknowledgements

This work is supported by National Key Research and Development Plan (Grant No. 2016YFC0303700), National Natural Science Foundation of China (Grant No. 51509258) and Science Foundation of China University of Petroleum, Beijing (No. 2462013YJRC003 and No. 2462015YQ0403).

References

An, C. and Su, J. (2011), "Dynamic response of clamped axially moving beams: Integral transform solution", *J. Appl. Math. Comput.*, **218**, 249-259.

An, C. and Su, J. (2014), "Dynamic response of axially moving Timoshenko beams: integral transform solution", *J. App. Math. Mech.(English Edition)*, **35**(11), 1421-1436

Bryndum, M.B. and Smed, P.F. (1998), "Application of the generalized force model for VIV in pipeline span design", *Proceedings of the OMAE 1998: 17th International Conference on Offshore Mechanics and Arctic Engineering*, Lisbon, Portugal.

Facchinettia, M.L., Langrea, E.D. and Biolley, F. (2004), "Coupling of structure and wake oscillators in vortex-induced vibrations", *J. Fluid. Struct.*, **19**(2), 123-140.

Furnes, G.K. and Berntsen, J. (2003), "On the response of a free span pipeline subjected to ocean currents", *J. Ocean Eng.*, **30**, 1553-1577.

Gu, J.J., An, C. and Levi, C. (2012), "Prediction of vortex-induced vibration of long flexible cylinders modeled by a coupled nonlinear oscillator: integral transform solution", *J. Hydrodynamics*, **24**(6), 888-898.

Gu, J.J., An, C., Duan, M.L., Levi, C. and Su, J. (2013), "Integral transform solutions of dynamic response of a clamped–clamped pipe conveying fluid", *J. Nucl.Eng. Design*, **254**(2013), 237-245

Guo, H.Y., Wang, S.Q., Wu, J.N. and Liu, D.F. (2000), "Dynamic characteristics of marine risers conveying fluid", *J. China Ocean Eng.*, **14**(2), 153-160.

Guo, H.Y., Wang, Y.B. and Fu, Q. (2004), "The effect of internal fluid on the response of vortex-induced vibration of marine rises", *J. China Ocean Eng.*, **18**(1), 11-20.

Iwan, W.D. (1981), "The vortex-induced oscillation of non-uniform structural systems", *J. Sound Vib.*, **79**(2), 291-301.

Lou, M., Ding, J., Guo, H. and Dong X. (2005), "Effect of internal flow on vortex-induced vibration of submarine free spanning pipelines", *J. China Ocean Eng.*, **19**, 147-154.

Ma, J.K., Su, J., Lu, C.H. and Li, J.M. (2006), "Integral transform solution of the transverse vibration of an axial moving string", *J. Vib. Measurement Diagnosis*, **26**, 104-107.

Pantazopoulos, M.S., Crossley, C.W., Orgill, G. and Lambrakos, K.F. (1993), "Fourier methodology for pipeline span vortex-induced vibration analysis in combined flow", *Proceedings of the International Conference on Offshore Mechanics and Arctic Engineering*, Glasgow, UK

Shen, Z.H. and Zhao, Q. (1996), "Effects of internal flow on vortex-induced vibration and fatigue life of submarine pipelines", *China Ocean Eng.*, **10**(3), 251-260

Wang, K., Tang, W. and Xue, H. (2014), "Cross-flow VIV-induced fatigue damage of deepwater steel catenary riser at touch-down point" *J. China Ocean Eng.*, **28**, 81-93.

Xie, L.W., Chen, G.M., Ju, S.D. and Xu, L.B. (2011), "VIV fatigue analysis program for submarine pipeline span", *J. Oil Field Equipment*, **40**(2), 1-4.

Xing, J.Z., Liu C.T. and Duan, M.L. (2005), "Vortex-induced vibration model of span segment of buried submarine pipeline", *Proceedings of the 5th (2005) International Offshore and Polar Engineering Conference*, Seoul, Korea.

Xu, T., Lauridsen, B. and Bai, Y. (1999), "Wave-induced fatigue of multi-span pipelines", *J. Marine Struct.*, **12**, 83-106.

Yang, B., Gao, F.P., Jeng, D.S. and Wu, Y.X. (2008), "Experimental study of vortex-induced vibrations of a pipeline near an erodible sandy seabed", *J. Ocean Eng.*, **35**(2008), 301-309.

MK